Urea-Hydroxyapatite Nanohybrids for Slow Release of Nitrogen

Nilwala Kottegoda,[†,‡] Chanaka Sandaruwan,[†] Gayan Priyadarshana,[†] Asitha Siriwardhana,[†] Upendra A. Rathnayake,[†] Danushka Madushanka Berugoda Arachchige,[†] Asurusinghe R. Kumarasinghe,[†,∥] Damayanthi Dahanayake,[†] Veranja Karunaratne,[†,§] and Gehan A. J. Amaratunga[*,†,⊥]

[†]Nanotechnology and Science Park, Center for Excellence in Nanotechnology, Sri Lanka Institute of Nanotechnology (SLINTEC), Mahenawatta, Pitipana, Homagama CO 10206, Sri Lanka

[‡]Department of Chemistry, University of Sri Jayewardenepura, Nugegoda 10250, Sri Lanka

[§]Department of Chemistry, University of Peradeniya, Peradeniya 20400, Sri Lanka

[∥]Faculty of Science and Technology, University of Uva Wellassa, Badulla 90000, Sri Lanka

[⊥]Department of Engineering, University of Cambridge, Trumpington Street, Cambridge CB2 1PZ, United Kingdom

Release study for Urea vs U-HA nanohybrid
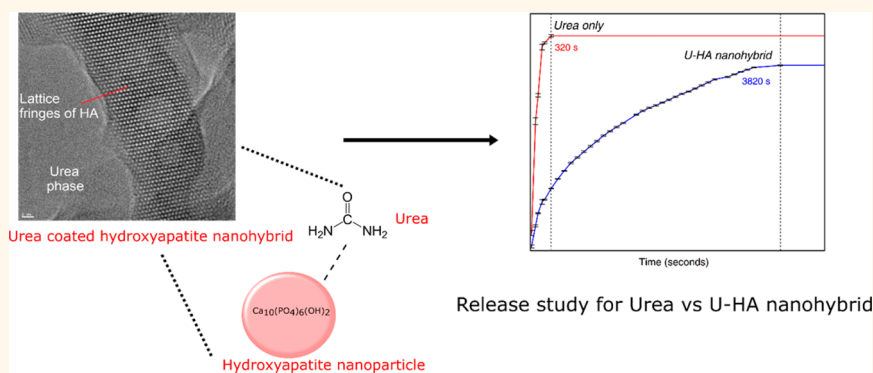
ABSTRACT: While slow release of chemicals has been widely applied for drug delivery, little work has been done on using this general nanotechnology-based principle for delivering nutrients to crops. In developing countries, the cost of fertilizers can be significant and is often the limiting factor for food supply. Thus, it is important to develop technologies that minimize the cost of fertilizers through efficient and targeted delivery. Urea is a rich source of nitrogen and therefore a commonly used fertilizer. We focus our work on the synthesis of environmentally benign nanoparticles carrying urea as the crop nutrient that can be released in a programmed manner for use as a nanofertilizer. In this study, the high solubility of urea molecules has been reduced by incorporating it into a matrix of hydroxyapatite nanoparticles. Hydroxyapatite nanoparticles have been selected due to their excellent biocompatibility while acting as a rich phosphorus source. In addition, the high surface area offered by nanoparticles allows binding of a large amount of urea molecules. The method reported here is simple and scalable, allowing the synthesis of a urea-modified hydroxyapatite nanohybrid as fertilizer having a ratio of urea to hydroxyapatite of 6:1 by weight. Specifically, a nanohybrid suspension was synthesized by *in situ* coating of hydroxyapatite with urea at the nanoscale. In addition to the stabilization imparted due to the high surface area to volume ratio of the nanoparticles, supplementary stabilization leading to high loading of urea was provided by flash drying the suspension to obtain a solid nanohybrid. This nanohybrid with a nitrogen weight of 40% provides a platform for its slow release. Its potential application in agriculture to maintain yield and reduce the amount of urea used is demonstrated.

KEYWORDS: urea-modified hydroxyapatite nanohybrid, nanoparticles, nitrogen fertilizer, slow release

Functional hybrid nanomaterials have received scientific interest because combinations of nanocomponents give rise to multifunctional properties due to synergistic effects from interfacial particle−particle interactions.[1] Hydroxyapatite [(Ca₁₀(PO₄)₆(OH)₂] nanoparticles (HA NPs) and their hybrids have been extensively studied because of their relevance in material science, biology, and medicine.[2,3] HA is the key constituent of human and animal hard tissues, and it is widely used as a bioceramic due to its biocompatibility.[4] Much of the literature on HA NPs is focused on its use in biomedical
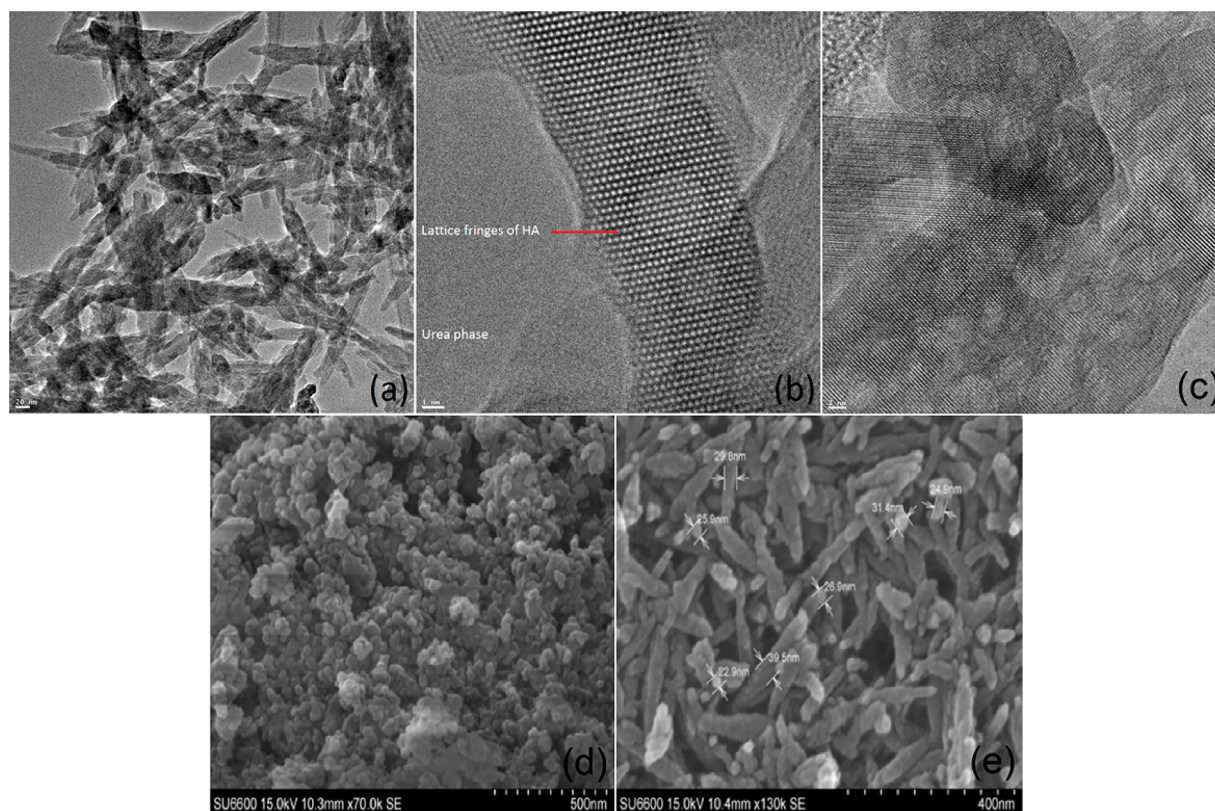
Figure 1. (a) TEM image of urea-HA nanohybrids showing the nanorod-like superstructure (scale bar represents 10 nm). (b) HRTEM image of urea-HA nanohybrid representing an internal structure of the urea-coated nanorod (scale bar represents 1 nm). (c) Hexagonal morphology of the urea-HA nanohybrids (scale bar represents 1 nm). SEM images showing the attachment of beads to form rod-like NPs: (d) bead-like NPs as synthesized and (e) formation of rod-like structures after spray drying.

applications,[5−8] whereas their potential agriculture applications have not been extensively studied[9] except for the work initiated in our laboratory.[10−17] However, naturally occurring rockphosphate, which is also a HA, is used traditionaly as a phosphorus fertilizer but has low solubility. Therefore, there is also increased possibility of P solubility to be achieved through a NP formulation. Furthermore, from a scientific point of view, the reactive surface functional groups on the HA NPs offer rich opportunities for surface modification through immobilization of strategic chemicals for creation of nanohybrids with multifunctional properties.

The Haber−Bosch process for the commercial production of ammonia demonstrated in 1913 was a watershed event in the mass production of nitrogen (N) fertilizers for modern agriculture. Today, nearly half the world population relies on the increased crop yields, especially wheat and rice, through the use of N fertilizers, the so-called "green revolution",[18] to access affordable food. Urea $[CO(NH_2)_2]$ is the principal N fertilizer (46% N by weight). However, the premature decomposition of urea in soil that occurs due to the action of water, volatilization, and urease enzyme leads to the evolution of ammonia before it can be efficiently adsorbed by the plants. This is a major challenge for global agriculture and threatens future food security.[19−22]

Here, we report a nanohybrid containing HA NPs decorated with urea in a 6:1 ratio (urea:HA NPs). Importantly, this nanohybrid displayed significant slow release of N. Based on our analyses, we infer that urea is weakly bound to HA NPs, owing to their high surface area to volume ratio and surface chemistry. The slow release of urea from this nanohybrid leads to a reduction in

the rate of urea decomposition in soil, therefore leading to higher N agronomic use efficiency (NAE)[23] of plants. We previously reported a urea-HA nanohybrid at a weight percent ratio of 1:1 that was incorporated into wood chips to achieve a slow release of urea and enhance yields of rice crops.[11] That process, while showing promise, was cumbersome, and the loading efficiency was low. In this work, we report a simpler approach to demonstrate the slow release of urea with six times higher loading. In depth structural studies of the urea-HA nanohybrids (6:1) reveal that weak interactions between HA NPs and urea are responsible for the slow release of urea.

Urea-HA nanohybrids were synthesized using a one-step in situ approach where H_3PO_4 (0.6 M, 250.0 cm^3) was added dropwise to a suspension containing $Ca(OH)_2$ (19.3 g, 250.0 cm^3) and urea (150.0 g). Subsequently, these mixtures were flash dried to obtain dry nanohybrids. Here, the presence of urea in the medium allows for its coating on HA NP as the nucleation occurs. Flash drying was used to form a dry nanohybrid and maintain the 6:1 urea to HA NP ratio from the suspension to the solid. It is noteworthy that traditional oven drying leads to phase separation. Furthermore, experimentation revealed that a loading at a ratio of 6:1 was the optimal concentration and an increase in urea concentration beyond this ratio led to phase separation even under flash drying. At this concentration and using flash drying, we were able to scale up the process to produce 87.5 kg of nanohybrids without compromising the properties (see Methods section).

RESULTS

A transmission electron microscopy (TEM) image (Figure 1a) of HA NPs shows rod-like NPs with diameters ranging from
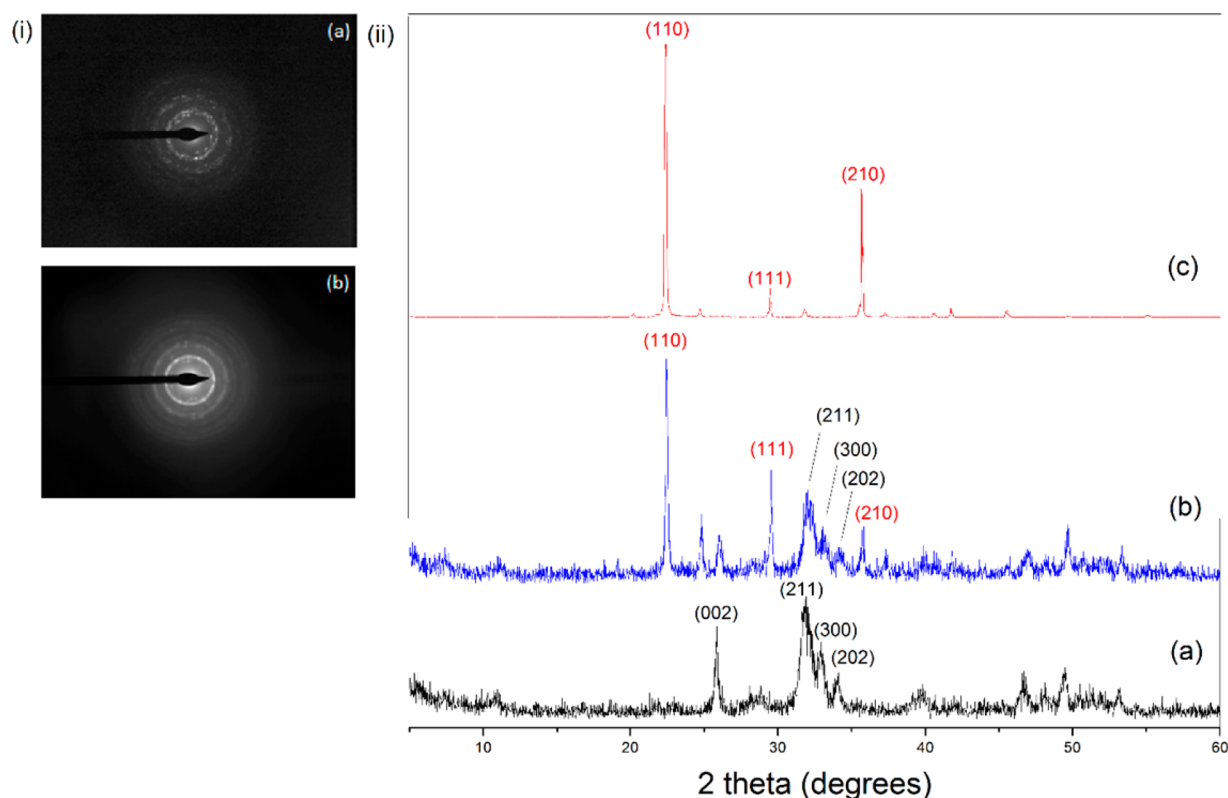
Figure 2. (i) Electron diffraction patterns of (a) urea and (b) urea-HA nanohybrids. (ii) PXRD patterns of (a) HA NPs, (b) urea-HA nanohybrids, and (c) urea.
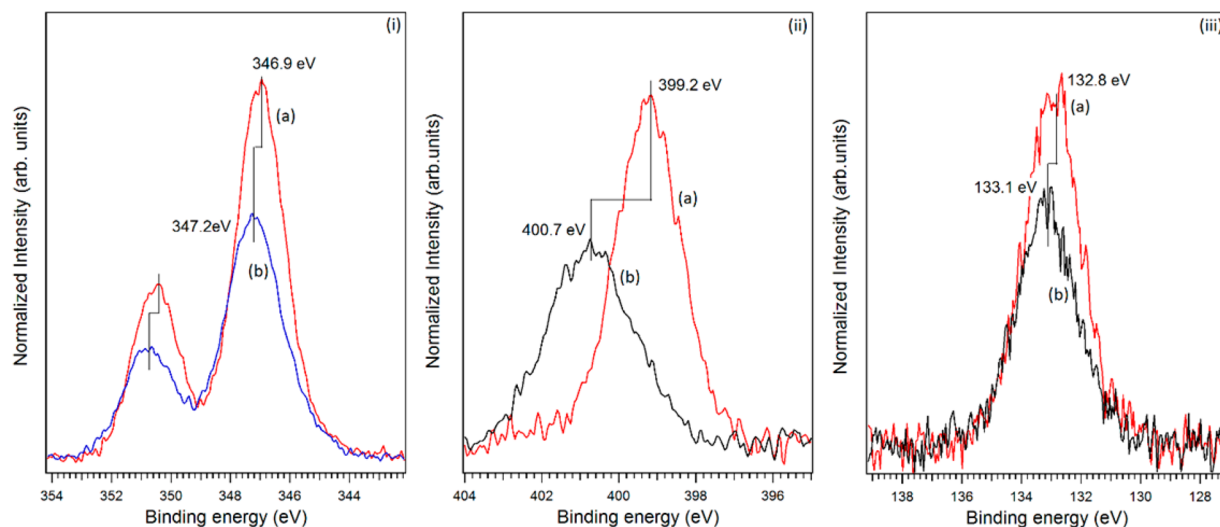

Figure 3. X-ray photoelectron spectra for (i) Ca 2p, (ii) N 2s and (iii) P 2p core levels of (a) HA NPs and (b) urea-HA nanohybrids.

15 to 20 nm and lengths from 100 to 200 nm. Closer TEM analyses reveal that the rods are coated with urea at nanoscale dimensions (Figure 1b). According to the scanning electron microscopy (SEM) analysis, initially nanobeads with dimensions of 5 nm are formed during the synthesis, followed by the attachment of beads to form rod-like NPs (Figure 1d,e).

As shown in Figure 1b, two distinct phases can be identified. The internal crystalline structures of urea-coated HA nanorods and self-assembled hexagonal morphology of HA NPs were observed. Here, crystal lattice planes are perfectly aligned with a lattice space of about 3.5 Å, corresponding to the interplanar

spacing of (002) planes for hexagonal HA (Figure 1c), suggesting that the growth of nanorods occurred in the (002) direction.

The polycrystalline nature of the HA NPs is evidenced by the selected area electron diffraction pattern and the broad and low intensity diffraction peak (002) in the powder X-ray diffraction (PXRD) pattern (Figure 2).

The crystallite size calculated using Scherer's formula was found to be ~18 nm, consistent with the TEM observations of the average size of bead-like NPs. We did not observe any shifts in the PXRD peak positions before and after HA NP surface modification, which suggests that the attachment of urea to the
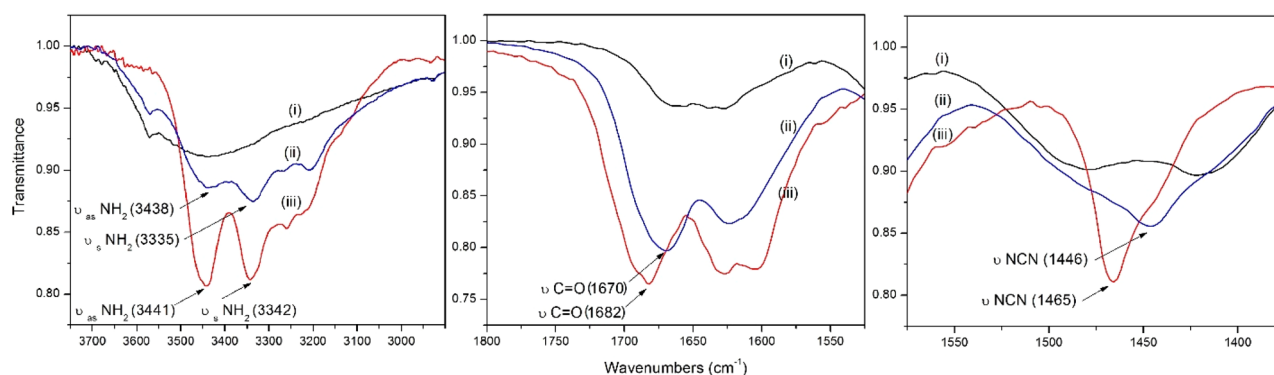
C

Figure 4. FTIR spectra of NH_2, C=O, and N−C−N regions of (i) HA NP (ii) urea-HA nanohybrid, and (iii) urea only.
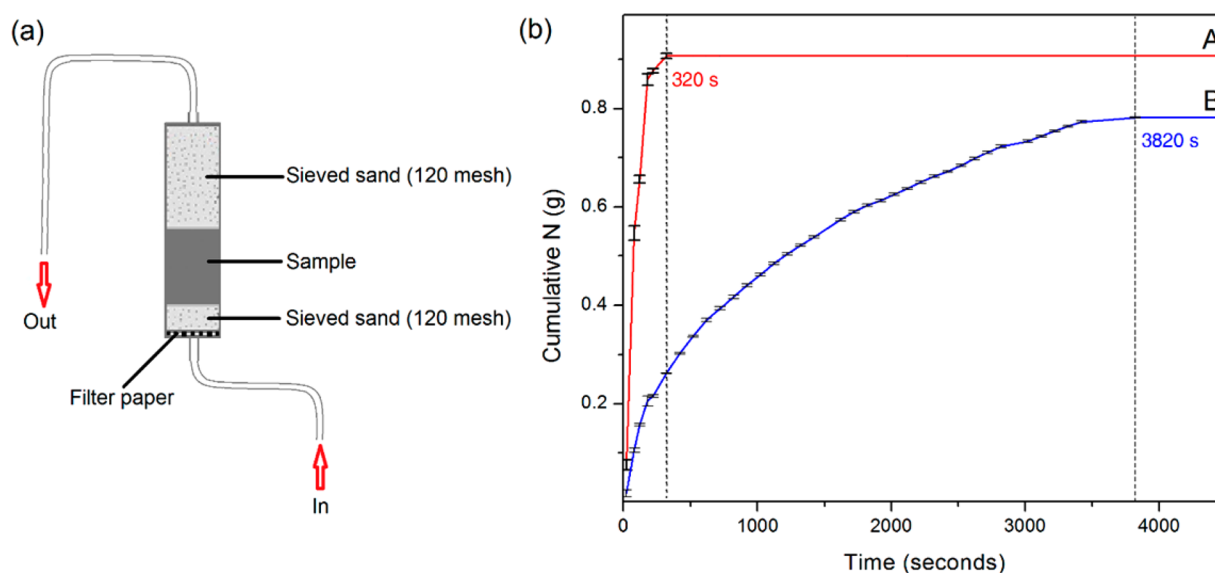

Figure 5. (a) Schematic representation of experimental setup for the dissolution studies. (b) Comparison of release behavior of (A) urea and (B) urea-HA nanohybrids (6:1) in water. The vertical line indicates the time to reach a constant value in cumulative N amounts in pure urea (99% of the initial amount used) and urea-HA nanohybrids (6:1) (86% of the initial amounts of urea-HA nanohybrid 6:1). In urea-HA nanohybrids, strongly bound urea, which released over longer periods time (up to 1 week), was detected, suggesting that urea encapsulated within the nanohybrid is available at different stages of release.

NPs is weak and the overall structure of HA NPs is not substantially modified.

We further studied the nature of interactions between the urea and HA NPs with X-ray photoelectron spectroscopy (XPS), as shown in Figure 3. More specifically, we monitored Ca 2p, N 1s, and the P 2p binding energies in pure HA NPs and the urea functionalized NPs.

It can be seen from Figure 3 that the most significant shift in the peak position toward higher binding energy was observed in the N 1s core level spectra of the urea-HA nanohybrid, indicating the formation of a new bond between urea and HA NPs through a N atom of urea. On the other hand, Ca 2p core level spectra of the urea-HA nanohybrid also show a noticeable shift toward higher binding energies when HA NPs are combined with urea. The shift in the binding energy of Ca 2p is significant for urea-HA nanohybrids, suggesting that the chemical environment around Ca^{2+} ions in HA has been modified due to the presence of urea molecules. Comparing the P 2p core level spectra for HA NPs and urea-HA nanohybrids, a shift in the peak position of P 2p core level of HA NPs toward a higher binding energy is observed when urea is attached to HA NPs, suggesting that the electron density around P has been influenced by the

introduction of urea into the system, possibly by forming H-bonds between phosphate groups of HA NPs and urea.

XPS data suggest that prominent bonding modes are the metal−ligand interactions between N atoms on urea and Ca atoms in HA NPs. FTIR characterization suggests that H-bonding modes are present as well. FTIR spectra (Figure 4) confirm that the N- and H-bonding environments in the urea-HA nanohybrids are altered compared to that of pure urea. Bonding of urea to HA through the N−H environments is also reflected as shifts in the N−C−N stretching and C=O regions. Taken together the FTIR and XPS data reveal that urea bonds to HA NPs through its carbonyl and amine modes.

In order to understand the change in the surface characteristics of HA NPs with the degree of urea functionalization, Brunauer−Emmett−Teller (BET) analysis was carried out for HA NPs and urea-HA nanohybrids with urea:HA NPs ratios of 1:1 and 6:1. N adsorption−desorption isotherms of the HA NPs and 1:1 urea-HA nanohybrids revealed a BET surface area of 81 and 56 $m^2\,g^{-1}$, respectively. According to the Barrett−Joyner−Helenda (BJH) method, the average particle volumes for HA NPs and urea-HA nanohybrid were calculated to be 0.28 $cm^3\,g^{-1}$ and 0.25 $cm^3\,g^{-1}$, respectively, with an average particle diameter of
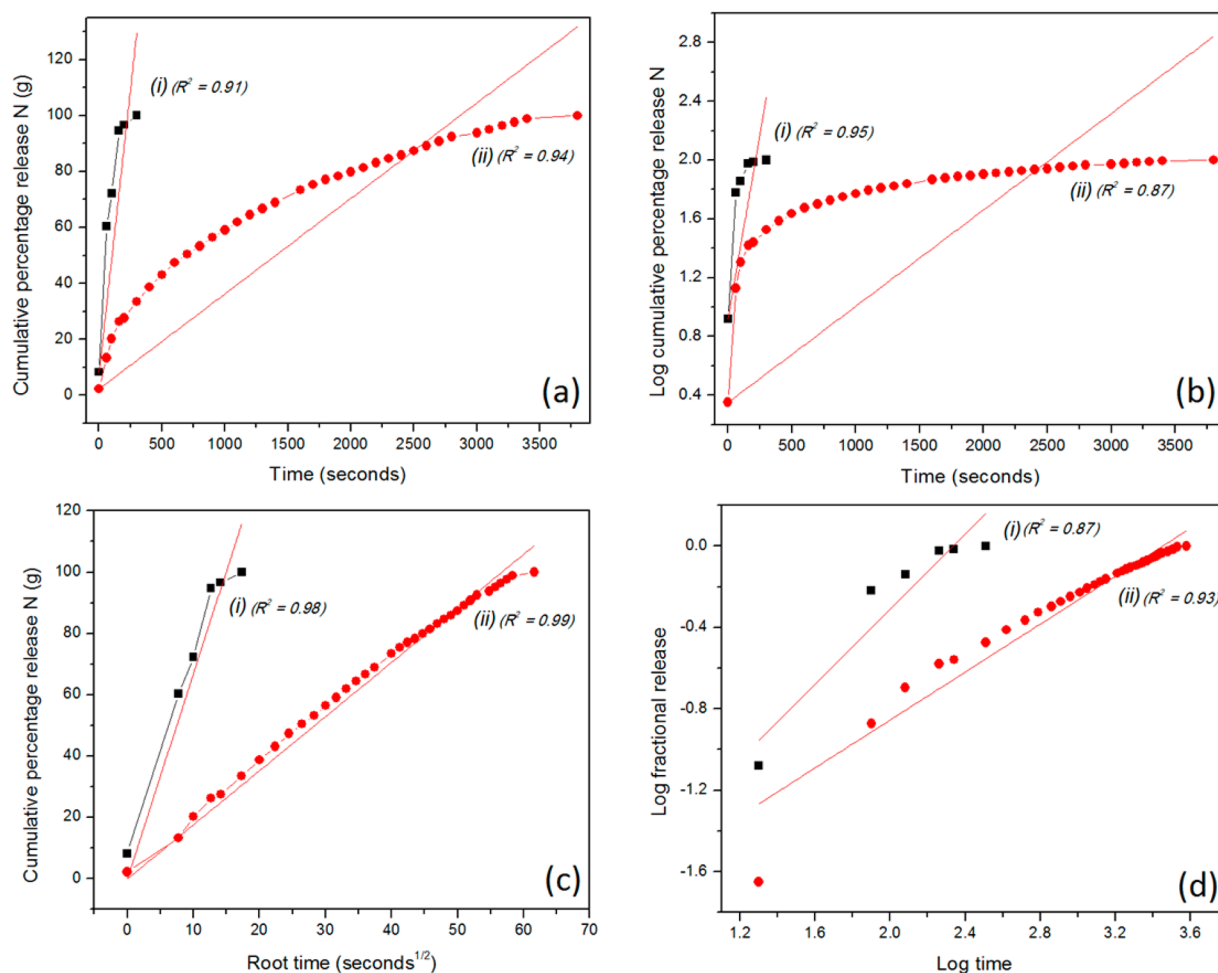
Figure 6. Comparison of the release kinetics of (i) urea and (ii) 6:1 ratio urea-HA nanohybrids in water using (a) zero-order kinetics, (b) first-order kinetics, (c) Higuchi model, and (d) Korsmeyer−Peppas model.

14 and 17 nm, respectively. The reduction of the surface area in urea-HA nanohybrids suggests successful surface modification. The BET surface area was reduced to 1.8 m^2 g^{-1} when the urea loading was increased up to a ratio of 6:1, thus confirming a greater coverage of HA NPs with urea. This is in agreement with the TEM micrographs showing a more uniform dispersion of HA NPs within the urea.

Nitrogen release behavior of the urea-HA nanohybrids in water was investigated using a rapid water release test using the set up given in the Figure 5a. Here, urea and urea-HA nanohybrid, each sample containing N amounts of 0.92 g, were placed in a column. Distilled water was then pumped from the bottom of the chamber at a rate of 3.75 mL/min, and water that elutes was collected at 20 s intervals continuously and analyzed using FT-IR spectroscopy (see Methods section). This test (Figure 5a) confirmed that the release rate was reduced by ~12 times compared to that of pure urea (Figure 5b).

In the rapid water release test, a fast burst release of pure urea (0.91 g out of 0.92 g or 99% of the N in urea) is seen within the first 320 s of exposure to water. On the other hand, significantly slow and sustained release of N is observed for 6:1 urea-HA nanohybrids (Figure 5b). Our measurements show that it took 3820 s to release 86% (or 0.79 g) of the N in urea in the 6:1 urea-HA nanohybrid. The rest of the 0.13 g (14%) of urea in the nanohybrids is released over a significantly longer period of time up to 1 week. For the urea-HA nanohybrids, the rate of release of

N was 12 times slower compared to pure urea, confirming the applicability of urea-HA nanohybrids as a slow release N source for agricultural applications. The slow release factor of N for this composite is comparable to that reported for urea-montmorillonite composites,[20,24] where the authors report release times of 1 h for urea versus 10 h for the composite according to their measurement method. The release profile of the nanohybrid is in agreement with the bonding mechanism suggested by several characterization techniques. Here, urea molecules are bound to HA NPs through a moderately strong bond which reduces the rate of release of urea. It is noteworthy that the bond between the two matrices is not too strong, such that the urea release rate is insufficient in practical applications.

The release kinetics of urea and urea-HA nanohybrid were studied with existing release models[25] using linear curve fitting and plotted to obtain rate constants and R^2 values (Figure 6). According to the R^2 values obtained, the Higuchi model which follows a Fickian diffusion gave the highest R^2 of 0.99 for urea-HA nanohybrids. Therefore, it can be surmised that the release mechanism is analogous to the release of water-soluble active molecules from a homogeneous matrix through diffusion in slow release drug formulations. In brief, urea is released from the nanohybrid through a diffusion-controlled mechanism according to Fickian kinetics. Accordingly, when the nanohybrid contacts soil moisture, depending on the pH value and the moisture level/ water level, urea releases from the hybrid in a slow and controlled

manner through a diffusion-controlled mechanism, leaving the NPs in the soil. There was no evidence of HA NPs entering into the plant.

The bioavailability of the slow release urea-HA nanohybrids was evaluated at the Rice Research and Development Institute of Sri Lanka, using rice as the model crop. The experiments were extended to field testing at certified farms, and it was observed that the urea-HA nanohybrids show tremendous promise for slow release. Initial trials on rice farms have revealed that a savings of up to 50% in urea consumption can be obtained by using urea-HA NP hybrids. The farm field trials were extended to three seasons, and a similar trend in crop yield improvement was observed (Figure 7).
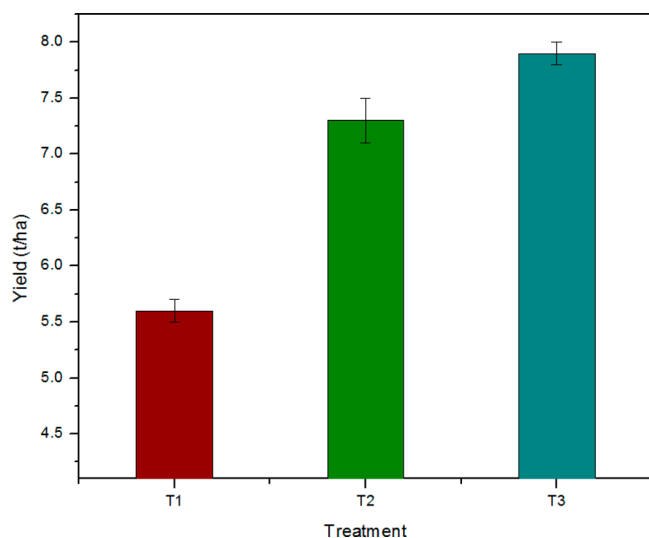

Figure 7. Crop yields at farmers field trials for no fertilizer (T1), granular urea according to the recommended amount: 100 kg of nitrogen/hectare (T2), and urea-HA nanohybrids at 50% of the recommended amount: 50 kg of nitrogen/hectare (T3).

The field trial data suggest that the nanohybrids can be translated directly to enhanced plant availability and growth while reducing the N content used by up to 50%. In the farm field trial data, 50% reduction in urea use allows the yield to be maintained at ∼7.9 tons/hectare, which is notably higher than the yields for the urea only rice crop yields (7.3 tons/hectare) using the recommended levels of urea. The NAE for the urea-HA nanohybrids is 48%, while the NAE for pure urea is 18%, at the field level.

Furthermore, the NPK contents in the leaves obtained from the rice paddy plants after 4 weeks of germination were compared for the recommended amount of urea added plants and 50% of the recommended urea as nanourea added plants. The results clearly show that there can be a 50% reduction in the amount of N applied and maintain plant uptake (see Table 1).

Table 1. NPK Content in the Leaf After 4 Weeks of Germination

treatment	N %	P % as P_2O_5	K% as K_2O
100% urea	2.53	0.015	0.55
50% urea as urea-HA nanohybrid	2.68	0.015	0.61

CONCLUSIONS

Our results suggest that functionalization of HA NPs with urea leads to a functional nanofertilizer. We have demonstrated that urea interacts with HA NPs by amine and carbonyl groups. This allows a slow release of nitrogen, an important nutrient for plants. The resulting urea-HA nanohybrids exhibit a slow release of N relative to pure urea. Release studies in a water medium show that the slow release can occur for up to 1 week in urea-HA NP nanohybrids, in contrast with pure urea which is expended within minutes. Finally, we correlate these slow release properties to a better rice crop yield at a 50% lower concentration of urea. This work demonstrates that nanotechnology can be used to develop slow release fertilizers which can significantly reduce the amount of chemicals used while maintaining yield.

METHODS

Materials. All reagents and chemicals used in this study, other than those for making the material for field trials, were purchased from the Sigma-Aldrich Company, USA, and were of analytical grade and used without further purification. All solutions were prepared using distilled water. The bulk nanofertilizer for field trials was made from industrial grade chemicals and reagents with solutions in tap water.

Synthesis of Urea-HA Nanohybrid (urea:HA Ratio 6:1); Scale Up Process. Solid urea (75 kg) was dissolved in a suspension of $Ca(OH)_2$ (9.65 kg, 75 L) and allowed to mix for 45 min. H_3PO_4 (0.6 M, 5.05 L) was added dropwise to the suspension, and the resulting composite with a urea:HA NP ratio of 6:1 was allowed to stir under mechanical agitation for a further 2 h. The resulting HA NP dispersion was dried using a flash drying technique at 60 °C to result in a urea-HA nanohybrid.

Release Behavior of the Urea-HA Nanohybrid in Water; Accelerated Test. Urea and urea-HA nanohybrid (6:1), each sample containing N amounts of 0.92 g, were placed in a column. Distilled water was then pumped from the bottom of the chamber at a rate of 3.75 mL/min, and water that elutes was collected at 20 s intervals continuously. Immediately after collecting, the samples were analyzed using FTIR spectroscopy and for the appearance of a characteristic urea N−C−N stretching peak in each sample: Bruker Vertex 80 coupled with Ram-FT module (RAM II) Fourier transform infrared (FT-IR) spectrophotometer in a range from 400 to 4000 cm^{-1} was used for quantitative analysis. The diffused reflectance FT-IR mode with potassium bromide (KBr) beam splitter and RT-DTGS detector was employed for solid samples, while the attenuated total reflectance (ATR) mode was used for liquid samples. A solid sample (0.5 mg) was mixed with spectroscopic grade KBr in a ratio of 1:500. For liquid samples, 20 μL of the sample was directly injected. The peaks were normalized with respect to an O−H stretching frequency peak of water, which did not shift, and the area under the peak was analyzed for a N−C−N stretching frequency peak of urea. Concentration of urea was determined using a calibration plot ranging from 0.2 to 2 M urea.

Farmers Field Trials for Rice. The experiments were carried out in a farmer's field after completing the pot and research plot trials. Experiments were carried out at Samanthurai, Sri Lanka during the months of September to December, 2015. The soil type at this geographical location is alluvial with an initial organic matter content of 1−3%, P (7−8 ppm) and K (130 ppm). Field trials were carried out following the randomized complete block design (RCBD) with each block having an area of 18 m^2. All the trials were carried out as triplicates.

Nitrogen fertilizer in the form of granular urea and urea-HA nanohybrid (6:1) were applied, and the results were compared to a no fertilizer applied control experiment. The bench mark value for N was 100 kg/ha. Except nitrogen, phosphorus (as P_2O_5, 37 kg/ha) and potassium (as K_2O, 45 kg/ha) nutrients were applied to each plot equally, following the recommendation of the Department of Agriculture (DOA), Sri Lanka, for the dry zone, and the standard agronomic practices were used. T1, no fertilizer; T2, granular urea (total of 100 kg/ha) as three applications at 2 week intervals after seeds were broadcasted, 30, 40, and 30 kg/ha, respectively; T3, urea-HA nanohybrid (6:1) (total of 50 kg/ha equal to 50% of DOA) as three applications at 2 week intervals after seeds were broadcasted, 15, 20, and

15 kg/ha, respectively. Leaf analysis was carried out for NPK content after 4 weeks of germination.

PXRD Studies. PXRD patterns of all synthesized samples were recorded using a Bruker D8 Focus X-ray powder diffractometer using Cu Kα radiation (λ= 0.154 nm) over a 2θ range of 3−65° with a step size of 0.02° and a step time of 1 s.

TEM. Transmission electron microscopic analysis was carried out using JEOL JEM 2100 microscope operating at 200 keV. The samples were dispersed in methanol using ultrasonication for 5 min. The suspended NPs were loaded on lacey carbon- coated copper grids (300 mesh), and the sample containing grids were dried for 24 h at room temperature prior to observation. Both imaging and selected area diffraction patterns were recorded.

SEM. Scanning electron microscopic analysis was carried out using a Hitachi SU 6600 scanning electron microscope. The images were recorded in the secondary electron mode, and the samples were coated with gold prior to analysis.

XPS. Solid samples (urea, urea-HA nanohybrid (6:1)) were spread evenly onto the surface of a conducting Cu (3M) tape to form a thin film composed of finely dispersed powder particles. Then, the loosely bound particles were blown off using a stream of dry N_2 gas. A monochromatic X-ray beam generating from an Al Kα source was used as the X-ray source. The binding energy scale of spectra was aligned to adventitious carbon at a binding energy (BE) of 284.5 eV, and the intensity was normalized to the number of scans. The background of the spectra was subtracted using a fourth-order polynomial function.

FTIR Spectroscopy. Bruker Vertex 80 coupled with Ram-FT module (RAM II) FTIR spectrophotometer in a range from 400 to 4000 cm^{-1} was used to determine the chemical structure and the bonding nature of the composites. A diffused reflectance FT-IR mode with potassium bromide (KBr) beam splitter and RT-DTGS detector was employed for solid samples, while an ATR mode was used for liquid samples.

BET Analysis. Surface areas of HA and urea-HA nanohybrid were analyzed using a Micrometrix, ASAP 2010 apparatus. A powdered sample (30 mg) was subjected to degassing at 573 K for overnight (∼16 h) prior to the analysis. All samples were oven-dried at 150 °C before degassing. After the degassing, microphore analysis was conducted for 48 h.

ICP-MS Analysis. A leaf K analysis was carried out using ICP-MS. The samples were digested according to USEPA 3050 standard. The measurements were taken using Agilent 7900 ICP-MS.

Leaf Nutrient Analysis. The leaf N content was measured using the standard Kjeldhal method.[26] Total P content was determined using the vanadomolybdate method,[27] and K was analyzed by ICP-MS measurements.

NAE. Nitrogen agronomic use efficiency was calculated as given below:

$$NAE(kg\ N\ kg^{-1}) = \text{yield from nitrogen treatment } (kg\ ha^{-1})$$
$$- \text{ yield from no nitrogen treatment } (kg\ ha^{-1})/\text{total nitrogen applied}$$
$$(kg\ ha^{-1})$$

AUTHOR INFORMATION

Corresponding Author
*E-mail: gehana@slintec.lk and gaja1@cam.ac.uk.

ORCID
Gehan A. J. Amaratunga: 0000-0002-8614-2864

Author Contributions
G.A.J.A. and V.K. mentored the project. N.K. developed the idea, designed the project, and provided the leadership for the team. N.K., C.S., G.P., A.S., U.A.R., B.A.D.M., and D.D. designed and performed the experiments and analyzed the data. A.R.K. performed XPS experiments.

Notes
The authors declare no competing financial interest.

REFERENCES

(1) Sanchez, C.; Boissiere, C.; Cassaignon, S.; Chaneac, C.; Durupthy, O.; Faustini, M.; Grosso, D.; Laberty-Robert, C.; Nicole, L.; Portehault, D.; et al. Molecular Engineering of Functional Inorganic and Hybrid Materials. *Chem. Mater.* **2014**, *26*, 221−238.

(2) Ferraz, M.; Monteiro, F.; Manuel, C. Hydroxyapatite Nanoparticles: A Review of Preparation Methodologies. *J. Appl. Biomater. Biom.* **2004**, *2*, 74−80.

(3) Zakaria, S. M.; Sharif Zein, S. H.; Othman, M. R.; Yang, F.; Jansen, J. A. Nanophase Hydroxyapatite as a Biomaterial in Advanced Hard Tissue Engineering: A Review. *Tissue Eng., Part B* **2013**, *19*, 431−441.

(4) Hua Cheng, Z.; Yasukawa, A.; Kandori, K.; Ishikawa, T. FTIR Study on Incorporation of CO_2 into Calcium Hydroxyapatite. *J. Chem. Soc., Faraday Trans.* **1998**, *94*, 1501−1505.

(5) Katti, S. K.; Katti, D. R.; Dash, R. Synthesis and Characterization of a Novel Chitosan/Montmorillonite/Hydroxyapatite Nanocomposite for Bone Tissue Engineering. *Biomed. Mater.* **2008**, *3*, 034122.

(6) Teng, S. H.; Lee, E. J.; Wang, P.; Jun, S. H.; Han, C. M.; Kim, H. E. Functionally Gradient Chitosan/Hydroxyapatite Composite Scaffolds for Controlled Drug Release. *J. Biomed. Mater. Res., Part B* **2009**, *90B*, 275−282.

(7) Mateus, A. Y. P.; Barrias, C. C.; Ribeiro, C.; Ferraz, M. P.; Monteiro, F. J. Comparative Study of Nanohydroxyapatite Microspheres for Medical Applications. *J. Biomed. Mater. Res., Part A* **2008**, *86A*, 483−493.

(8) Ferraz, M. P.; Mateus, A. Y.; Sousa, J. C.; Monteiro, F. J. Nanohydroxyapatite Microspheres as Delivery System for Antibiotics: Release Kinetics, Antimicrobial Activity, and Interaction with Osteoblasts. *J. Biomed. Mater. Res., Part A* **2007**, *81A*, 994−1004.

(9) Giroto, A.; Fidélis, S.; Ribeiro, C. Controlled Release from Hydroxyapatite Nanoparticles Incorporated into Biodegradable, Soluble Host Matrixes. *RSC Adv.* **2015**, *5*, 104179−104186.

(10) Gunaratne, G. P.; Kottegoda, N.; Madusanka, N.; Munaweera, I.; Sandaruwan, C.; Priyadarshana, W. M. G. I.; Siriwardhana, A.; Madhushanka, B. A. D.; Rathnayake, U. A.; Karunaratne, V. Two New Plant Nutrient Nanocomposites Based on Urea Coated Hydroxyapatite: Efficacy and Plant Uptake. *Indian J. Agric. Sci.* **2016**, *86*, 4.

(11) Kottegoda, N.; Munaweera, I.; Madusanka, N.; Karunaratne, V. A Green Slow-Release Fertilizer Composition Based on Urea-Modified Hydroxyapatite Nanoparticles Encapsulated Wood. *Curr. Sci.* **2011**, *101*, 6.

(12) Kottegoda, N.; Munaweera, I.; Madusanka, N.; Sirisena, D.; DIssanayake, N.; Amaratunga, G. A. J.; Karunaratne, V. The Advent of Nanotechnology in Smart Fertilizer, World Agriculture. *World Agric.* **2012**, *3*, 5.

(13) Kottegoda, N.; Munaweera, I.; Madusanka, N. A.; Karunaratne, V. Compositions for Sustained Release of Agricultural Macronutrients and Process thereof. US Patent 8361185, 2013.

(14) Kottegoda, N.; Munaweera, I.; Samaranayake, L.; Gunasekara, S.; De Alwis, A.; Karunaratne, V.; Madusanka, A. N. Cellulose based Sustained Release Macronutrient Composition for Fertilizer Application. US Patent 8617284, December 31, 2013.

(15) Kottegoda, N.; Priyadharshana, G.; Sandaruwan, C.; Dahanayake, D.; Gunasekara, S.; Amaratunga, G. A. J.; Karunaratne, V. Composition and Method for Sustained Release of Agricultural Macronutrients. US Patent 8696784, April 15, 2014.

(16) Kottegoda, N.; Sandaruwan, C.; Perera, P.; Madusanka, N.; Karunaratne, V. Modified Layered Nanohybrid Structures for The Slow Release of Urea. *Nanosci. Nanotechnol.–Asia* **2015**, *4*, 94.

(17) Kottegoda, N.; Siriwardhana, D.; Priyadarshana, G.; Sandaruwan, C.; Madushanka, B.; Rathnayake, U.; Gunasekara, S.; Dahanayake, D.; DeAlwis, A.; Kumarasinghe, A. Compositions and Methods for Sustained Release of Agricultural Macronutrients. US Patent Application US20140165683, June 19, 2014.

(18) Borlaug, N. E. *The Green Revolution Revisited and the Road Ahead*; Nobelprize.org; Nobel Media AB: Stockholm, Sweden, access date: 26 September 2002.

(19) DeRosa, M. C.; Monreal, C.; Schnitzer, M.; Walsh, R.; Sultan, Y. Nanotechnology in Fertilizers. *Nat. Nanotechnol.* **2010**, *5*, 91.

(20) Park, M.; Kim, C. Y.; Lee, D. H.; Choi, C. L.; Choi, J.; Lee, S. R.; Choy, J. H. Intercalation of Magnesium−Urea Complex into Swelling Clay. *J. Phys. Chem. Solids* **2004**, *65*, 409−412.

(21) Torres-Dorante, L.; Lammel, J.; Kuhlmann, H. Use of a Layered Double Hydroxide (LDH) to Buffer Nitrate In Soil: Long-Term Nitrate Exchange Properties Under Cropping and Fallow Conditions. *Plant Soil* **2009**, *315*, 257−272.

(22) Karunaratne, V.; Kottegoda, N.; De Alwis, A. Nanotechnology in a World Out of Balance. *J. Natl. Sci. Found. Sri Lanka* **2012**, *40*, 3−8.

(23) Gao, X.; Li, C.; Zhang, M.; Wang, R.; Chen, B. Controlled Release Urea Improved the Nitrogen Use Efficiency, Yield and Quality of Potato (Solanum Tuberosum L.) on Silt Loamy Soil. *Field Crop Res.* **2015**, *181*, 60−68.

(24) Pereira, E. I.; Minussi, F. B.; da Cruz, C. C.; Bernardi, A. C.; Ribeiro, C. Urea−Montmorillonite-Extruded Nanocomposites: A Novel Slow-Release Material. *J. Agric. Food Chem.* **2012**, *60*, 5267−5272.

(25) Costa, P.; Sousa Lobo, J. M. Modeling and Comparison of Dissolution Profiles. *Eur. J. Pharm. Sci.* **2001**, *13*, 123−133.

(26) Bremner, J. M.; Mulvaney, C. S. Nitrogen-Total. In *Methods of Soil Analysis. Part 2*; Page, A. L.; Miller, R. H.; Keeney, D. R., Eds.; American Society of Agronomy: Madison, WI, 1982; pp 595−624.

(27) *Sri Lanka Standards 645: Determination of Phosphorous Content, Part 5*; Sri Lanka Accreditation Board for Conformity Assessment: Colombo, Sri Lanka, 1985.